

Efficient steam generation by inexpensive narrow gap evaporation device for solar applications

Original

Efficient steam generation by inexpensive narrow gap evaporation device for solar applications / Morciano, Matteo; Fasano, Matteo; Salomov, Uktam; Ventola, Luigi; Chiavazzo, Eliodoro; Asinari, Pietro. - In: SCIENTIFIC REPORTS. - ISSN 2045-2322. - ELETTRONICO. - 7:1(2017), p. 11970. [10.1038/s41598-017-12152-6]

Availability:

This version is available at: 11583/2681606 since: 2017-09-22T12:43:51Z

Publisher:

Nature

Published

DOI:10.1038/s41598-017-12152-6

Terms of use:

This article is made available under terms and conditions as specified in the corresponding bibliographic description in the repository

Publisher copyright

(Article begins on next page)



Contents lists available at ScienceDirect

Journal of Cystic Fibrosis

journal homepage: www.elsevier.com/locate/jcf

Original Article

Immune response of polarized cystic fibrosis airway epithelial cells infected with Influenza A virus

Aderonke Sofoluwe^a, Alice Zoso^{a,1}, Marc Bacchetta^a, Sylvain Lemeille^b, Marc Chanson^{a,*}^a Faculty of Medicine, Department of Cell Physiology & Metabolism, University of Geneva, Geneva, Switzerland^b Faculty of Medicine, Department of Pathology & Immunology, University of Geneva, Geneva, Switzerland

ARTICLE INFO

Article history:

Received 21 May 2020

Revised 5 August 2020

Accepted 23 August 2020

Available online xxx

Keywords:

Immune response

Cystic fibrosis

Transcriptome

Airway epithelium

Pathogens

ABSTRACT

Background: Cystic fibrosis (CF), a genetic disease caused by mutations of the cystic fibrosis transmembrane conductance regulator (CFTR) gene, is characterized by dysfunction of the immune response in the airway epithelium that leads to prolonged infection, colonization and exacerbated inflammation. In this study, we determined the gene expression profile of airway epithelial cells knockdown for CFTR (CFTR KD) in response to bacterial and viral challenges.

Methods: In a first approach, polarized CFTR KD and their control counterpart (CFTR CTL) cells were stimulated with *P. aeruginosa*-derived virulence factor flagellin. Next, we developed a model of Influenza A virus (IAV) infection in CTL and CFTR KD polarized cells. mRNA was collected for transcriptome analysis.

Results: Beside the expected pro-inflammatory response, Gene Set Enrichment Analysis highlighted key molecular pathways and players involved in IAV and anti-viral interferon signaling. Although IAV replication was similar in both cell types, multiplex gene expression analysis revealed changes of key immune genes dependent on time of infection that were found to be CFTR-dependent and/or IAV-dependent. Interferons are key signaling proteins/cytokines in the antibacterial and antiviral response. To evaluate their impact on the altered gene expression profile in CFTR responses to pathogens, we measured transcriptome changes after exposure to Type I-, Type II- and Type III-interferons.

Conclusions: Our findings reveal target genes in understanding the defective immune response in the CF airway epithelium in the context of viral infection. Information provided in this study would be useful to understand the dysfunctional immune response of the CF airway epithelium during infection.

© 2020 The Author(s). Published by Elsevier B.V. on behalf of European Cystic Fibrosis Society. This is an open access article under the CC BY license. (<http://creativecommons.org/licenses/by/4.0/>)

1. Introduction

Cystic fibrosis (CF) is caused by mutations in the gene encoding the cystic fibrosis transmembrane conductance regulator (CFTR), a chloride ion channel that has an impact on airway surface hydration, mucociliary clearance, polymicrobial infections and inflammation. Complex bacterial communities, including opportunistic pathogens like *Pseudomonas aeruginosa* and *Staphylococcus aureus*, are common in airways of CF patients and the contribution of the CF microbiome to the airway disease is under investigation [1]. Although the molecular mechanisms underlying the disease have been elucidated, early events in the anamnesis of CF patients that

might determine the clinical path of disease development are less understood.

Respiratory viral infections of the airway are known to alter the clinical status of patients with CF [2,3]. Nasal airway surface liquid deficiency has been recently described to counteract viral infection in the new-born CF pig [4]. Influenza A virus (IAV) is a common human respiratory pathogen causing seasonal "flu", which mainly affects children, the elderly and immunocompromised patients [5], but also patients with chronic respiratory disease. A major complication of IAV infection is bacterial superinfection, whereby an initial viral infection primes the airway epithelium for a secondary severe bacterial infection that exacerbates lung inflammation and damage [6]. Recent studies have demonstrated a positive correlation between virus presence and a higher prevalence of traditional CF pathogens such as *P. aeruginosa* and *S. aureus* [7]. These reports suggest the importance of respiratory viral infections as risk factors for CF lung disease progression.

* Corresponding author at: Department of Cell Physiology & Metabolism, Medical School Center 1, Rue Michel-Servet, 1211 Geneva, Switzerland.

E-mail address: marc.chanson@unige.ch (M. Chanson).

¹ Present address: Department of Mechanical and Aerospace Engineering, Politecnico di Torino, Torino, Italy.

<https://doi.org/10.1016/j.jcf.2020.08.012>

1569-1993/© 2020 The Author(s). Published by Elsevier B.V. on behalf of European Cystic Fibrosis Society. This is an open access article under the CC BY license. (<http://creativecommons.org/licenses/by/4.0/>)

Please cite this article as: A. Sofoluwe, A. Zoso and M. Bacchetta et al., Immune response of polarized cystic fibrosis airway epithelial cells infected with Influenza A virus, Journal of Cystic Fibrosis, <https://doi.org/10.1016/j.jcf.2020.08.012>

In the CF lungs, pathogens outcompete each other causing infections with prolonged inflammation that creates irreversible lung damage. New strategies for early treatment of infection in CF patients are thus essential to reduce the morbidity of this lung disease. Here, we used a recently established airway epithelial cell model and transcriptomic analysis to investigate the immune response after *P. aeruginosa*-derived flagellin stimulation, IAV infection and the response to interferons (IFNs) after *CFTR* silencing.

2. Methods

2.1. Cell culture and transduction

The detailed procedure is provided in the supplementary Materials and Methods. Briefly, Human airway epithelial Calu-3 cells (ATCC® HTB-55™) were transduced with CRISPR lentiviral vector particles containing Cas9-HA-GFP sequence and single-guide RNA targeting *CFTR* exon 2 to generate *CFTR* Control (*CFTR* CTL) and *CFTR* knockdown (*CFTR* KD) cells [8]. 10^5 cells were transferred on 0.33 cm² Transwell filters (Corning, #3470) and cultured for 14–21 days to generate polarized epithelium.

2.2. RNA-seq analysis and qPCR

mRNA was collected from samples with various treatments. The procedure is provided in the Supplementary Materials and Methods. Analysis was performed as described [9]. qPCR was performed using SYBR primers (Supplementary Table 1).

2.3. Virus infection and plaque assay

Polarized *CFTR* KD and counterparts were infected with IAV at a multiplicity of infection (MOI) 0.05. Apical medium from samples were collected, plaque assays were performed and analyzed according to the protocol described in the Supplementary Materials and Methods.

2.4. Transcription factor pathway analysis

The network of interactions between transcription factors and target genes, based upon Reactome repositories, was performed with NetworkAnalyst (<http://www.networkanalyst.ca/>), using the Jasper database.

2.5. Statistical analysis

Statistical analyses were performed using Prism 8.0.2 (Graph Pad Prism) with data expressed as mean \pm standard error of the mean (SEM). One-way ANOVA or student t test were used for analysis. $*p \leq 0.05$, $**p \leq 0.01$, $***p \leq 0.001$ were considered significant. Heat maps of differentially expressed genes were generated with Prism software.

3. Results

3.1. *CFTR* inhibition in Calu-3 cells reveals dysregulated immune response with flagellin stimulation

The knockdown of *CFTR* by CRISPR-Cas9 in the Calu-3 submucosal gland airway epithelial cell line (*CFTR* KD) has been previously described [8]. To investigate the consequence of *CFTR* deletion on global gene expression, we compared the transcriptomic profiles of polarized *CFTR* CTL and *CFTR* KD stimulated with or without flagellin. *P. aeruginosa*-derived flagellin (virulence factor)

was used to mimic *P. aeruginosa* infection and stimulate an inflammatory host response. The experiment was performed in duplicates, multi-dimensional scaling plots reveals the similarities between the samples used (Supplementary Fig. 1A). Distances on the plot represent coefficient of variation in expression between samples. The differential expression analysis was performed for the genes annotated in hg19 and the counts were normalized according to the library size and filtered. We obtained 23,420 raw gene numbers, the differential expressed gene (DEG) counts are provided in Supplementary Table 2. Supplementary Fig. 1B shows the distribution of the DEGs across the sample sets, revealing the commonly expressed and uniquely expressed genes in our non-stimulated (NS) or flagellin-stimulated (F) samples (CTL_NS vs KD_NS-green, CTL_F vs KD_F-yellow, CTL_NS vs CTL_F-pink and KD_NS vs KD_F-violet). Heat maps also show the changes in the expression of genes in *CFTR* CTL and *CFTR* KD unstimulated cells or when stimulated with flagellin (Supplementary Fig. 1C) for the duplicate experiments.

PANTHER analysis revealed protein classes that include “cell adhesion molecule”, “extracellular matrix”, “structural protein” in the comparison between unstimulated *CFTR* CTL and *CFTR* KD cells. Interestingly, PANTHER analysis revealed protein classes that were associated with the immune response, which include “signaling molecule”, “defense immunity”, “transmembrane receptor regulatory/adaptor protein” in the comparison between flagellin-stimulated *CFTR* CTL and *CFTR* KD cells (Fig. 1A and B). Volcano plots showed that flagellin stimulation induced important gene expression changes in both *CFTR* CTL and *CFTR* KD cells (Fig. 1C and D), although the transcriptome response appeared fairly similar between the two cell lines (red dots-upregulated genes in non-stimulated cells, blue dots-upregulated genes in flagellin-stimulated cells). Not surprisingly, Gene Set Enrichment Analysis (GSEA) predicted pathways associated with inflammation, including “cytokine-cytokine receptor interaction”, “TNF signaling”, “NF- κ B signaling”, Toll-like receptor” or “IL-1 signaling” in both *CFTR* CTL and *CFTR* KD cells exposed to flagellin (Fig. 1E).

Less expected pathways, usually associated with viral infection, were also enriched such as “Influenza A”, “JAK/STAT signaling”, “RIG-I like receptor signaling”, “Type-II IFN signaling”, “NOD like receptor signaling” or “Type-I IFN signaling” (Fig. 1F). Interestingly, GSEA of the flagellin-induced pathways between *CFTR* CTL and *CFTR* KD cells suggested up-regulation and down-regulation of some “pro-inflammatory” and “viral-associated” pathways, respectively (Fig. 1G). A list of the genes contributing to these pathways is provided in Supplementary Table 3. Hence, flagellin stimulation revealed potential dysregulation of signaling pathways involved in defense against viral infection.

3.2. IAV infection of *CFTR* CTL and *CFTR* KD cells

The RNA-seq data prompted us to develop a protocol to monitor viral infection with Influenza A virus. To this end, *CFTR* CTL and *CFTR* KD cells grown on Transwell filters were infected at MOI 0.05 with IAV PR8 (H1N1) and monitored up to 72 h. As shown in Fig. 2A, the release of virus particles was detected 18 h post-infection by plaque assay and reached a plateau after 24 h. These results were confirmed by the detection of the IAV nucleoprotein (NP) by Western blot (Fig. 2B). We observed a slight increase in IAV NP in *CFTR* KD cells that was however not reflected in the measurement of virus particle release using plaque assays. We also evaluated whether the integrity of the *CFTR* CTL and *CFTR* KD epithelium was affected by IAV infection by measuring the transepithelial electrical resistance (TEER). TEER dropped in both cell lines 48 h post-infection (Fig. 2C). Infection was also verified with immunofluorescence detection of the IAV nuclear protein (Fig. 2D).

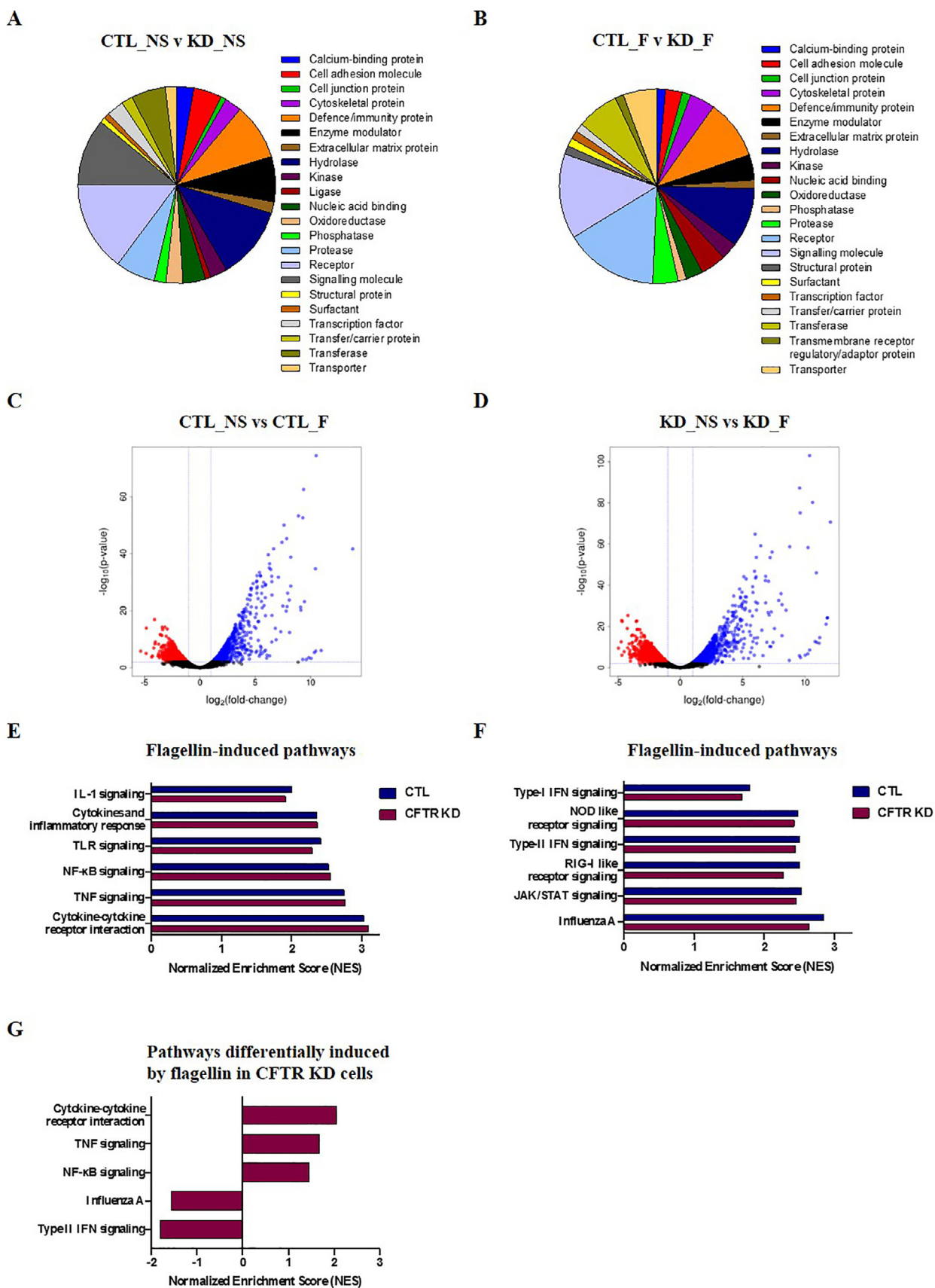


Fig. 1. Transcriptomic profile of flagellin CFTR CTL and CFTR KD stimulated cells. Pie Charts representing PANTHER Protein Class analysis in (A) CTL_NS vs KD_NS and (B) CTL_F vs KD_F conditions. (C) Volcano plots showing differentially expressed genes in CTL_NS v CTL_F conditions (D) and KD_NS v KD_F conditions (blue- upregulated in flagellin-stimulated cells, red-upregulated in non-stimulated cells). (E, F) Bar charts showing normalized enrichment scores of flagellin pathways in CFTR CTL (blue) and CFTR KD cells (red). (G) Bar chart showing normalized enrichment scores of flagellin pathways differentially modulated in CFTR KD cells as compared to CFTR CTL cells. (For interpretation of the references to color in this figure legend, the reader is referred to the web version of this article.)

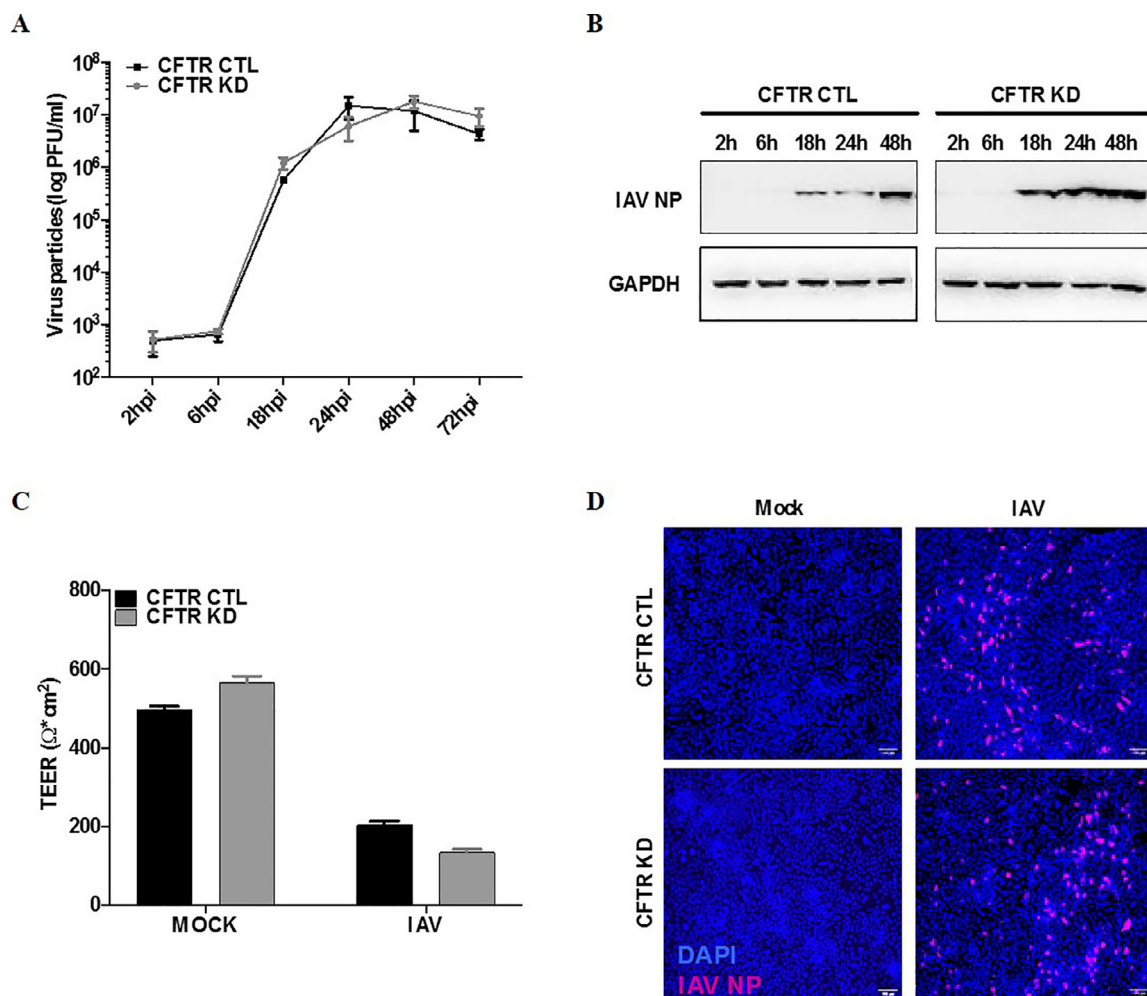


Fig. 2. IAV infection of CFTR CTL and CFTR KD cells. (A) Viral titer analysis of IAV infected CFTR CTL and CFTR KD cells 2, 6, 18, 24, 48 and 72 h post infection (hpi), MOI 0.05 (n=6). (B) Western blot showing IAV nuclear protein (NP) expression 2, 6, 18, 24 and 48 hpi. (C) Transepithelial electrical resistance (TEER) measurements of mock and IAV infected CFTR CTL (black) and CFTR KD (grey) cells at 48 hpi. (D) Immunofluorescence of IAV NP (magenta) and histocompatibility complex antigen receptors (HLA-DPA1, HLA-DPB1, HLA-DQA1) in both cell types. Compared to control cells, CFTR KD cells exhibited gene expression differences under basal and/or IAV-infected conditions. Fig. 4A shows a heat map of the genes with fold-changes of their expression below or above 2. The effect of CFTR knockdown on gene expression changes in uninfected cells can be appreciated when comparing KD mock versus CTL mock conditions in Fig. 4A (last column). For example, *BCL2*, *CYBB/NOX2*, *IL11RA*, *IRF5* and *TLR9* were downregulated (blue arrows) in CFTR KD cells while *CCL2/MCP1* and *DEFB4A* (β -defensin2) were upregulated (red arrows). Interestingly, there are genes in CFTR KD cells that also show differences in their expression as compared to CFTR CTL cells during IAV infection. These include *CCL13/MCP4*, *CD1D*, *CD22*, *CIITA*, *GBP5*, *IL18R1*, *IL1A*, *IL2RG*, *LCP2*, *LY96*, *NLRP3*, *TBX21*, *TNF*, *TNFRSF1B*, *XCL1* and *ZEB1* (Fig. 4A). *CCL2* and *CCL5*, the expression of which is affected by CFTR silencing, were also differently modulated between CTL and CFTR KD cells infected by IAV.

Thus, no apparent difference in virus particle processing was observed between CFTR KD and CFTR CTL cells.

To gain insights in the immune response of CFTR CTL and CFTR KD cells to IAV infection, we used a multiplex gene expression analysis with a panel of 579 immunology related genes. Relative changes of gene expression in response to time (24, 48 and 72 h) of viral (V) infection in both cell lines (CTL V24, CTL V48, CTL V72 and KD V24, KD V48, KD V72) was normalized to uninfected CTL cells (CTL Mock). Venn diagrams illustrating the unique and common genes modulated by IAV infection between CFTR CTL and CFTR KD cells is shown in Supplementary Fig. 2. Fig. 3A shows the distribution of fold changes (Log₂FC) in gene expression for all conditions. Using qPCR, we confirmed the expression of key marker genes of the response to viral infection at 48h, including IL-8 (*CXCL8*), IL-6 and *IP10* (*CXCL10*) (Fig. 3B–D). mRNA of the M1 protein, which plays a critical role in virus replication, was monitored as a control of infection (Fig. 3E). As shown in Fig. 3, mRNAs for these genes were strongly induced in both cell lines but to similar extent, suggesting that the host-response to viral infection was apparently not different between CFTR CTL and CFTR KD cells.

3.3. Immune gene profile of CFTR KD cells induced by IAV infection

Supplementary Table 4 shows all gene expression changes in response to IAV infection of CFTR CTL and CFTR KD cells. IAV induced at all-time points strong expression of genes

typical of viral responses, including C-C motif (*CCL20/MIP3 α* , *CCL22*) and C-X-C motif (*CXCL10/IP10*) chemokines, IFNs (*IFN β 1*, *IL29/IFN λ 3*, *IL28A/IFN λ 2*, *IL28A/B/IFN λ*), IFN-associated molecules (*BST2/Tetherin*, *CXCL11/I-TAC*) and histocompatibility complex antigen receptors (*HLA-DPA1*, *HLA-DPB1*, *HLA-DQA1*) in both cell types. Compared to control cells, CFTR KD cells exhibited gene expression differences under basal and/or IAV-infected conditions. Fig. 4A shows a heat map of the genes with fold-changes of their expression below or above 2. The effect of CFTR knockdown on gene expression changes in uninfected cells can be appreciated when comparing KD mock versus CTL mock conditions in Fig. 4A (last column). For example, *BCL2*, *CYBB/NOX2*, *IL11RA*, *IRF5* and *TLR9* were downregulated (blue arrows) in CFTR KD cells while *CCL2/MCP1* and *DEFB4A* (β -defensin2) were upregulated (red arrows). Interestingly, there are genes in CFTR KD cells that also show differences in their expression as compared to CFTR CTL cells during IAV infection. These include *CCL13/MCP4*, *CD1D*, *CD22*, *CIITA*, *GBP5*, *IL18R1*, *IL1A*, *IL2RG*, *LCP2*, *LY96*, *NLRP3*, *TBX21*, *TNF*, *TNFRSF1B*, *XCL1* and *ZEB1* (Fig. 4A). *CCL2* and *CCL5*, the expression of which is affected by CFTR silencing, were also differently modulated between CTL and CFTR KD cells infected by IAV.

3.4. Immune gene profile induced by IFN in CFTR KD cells

Altered signaling of CF airway epithelial cells in response to IFN has been reported in various studies. This was also predicted

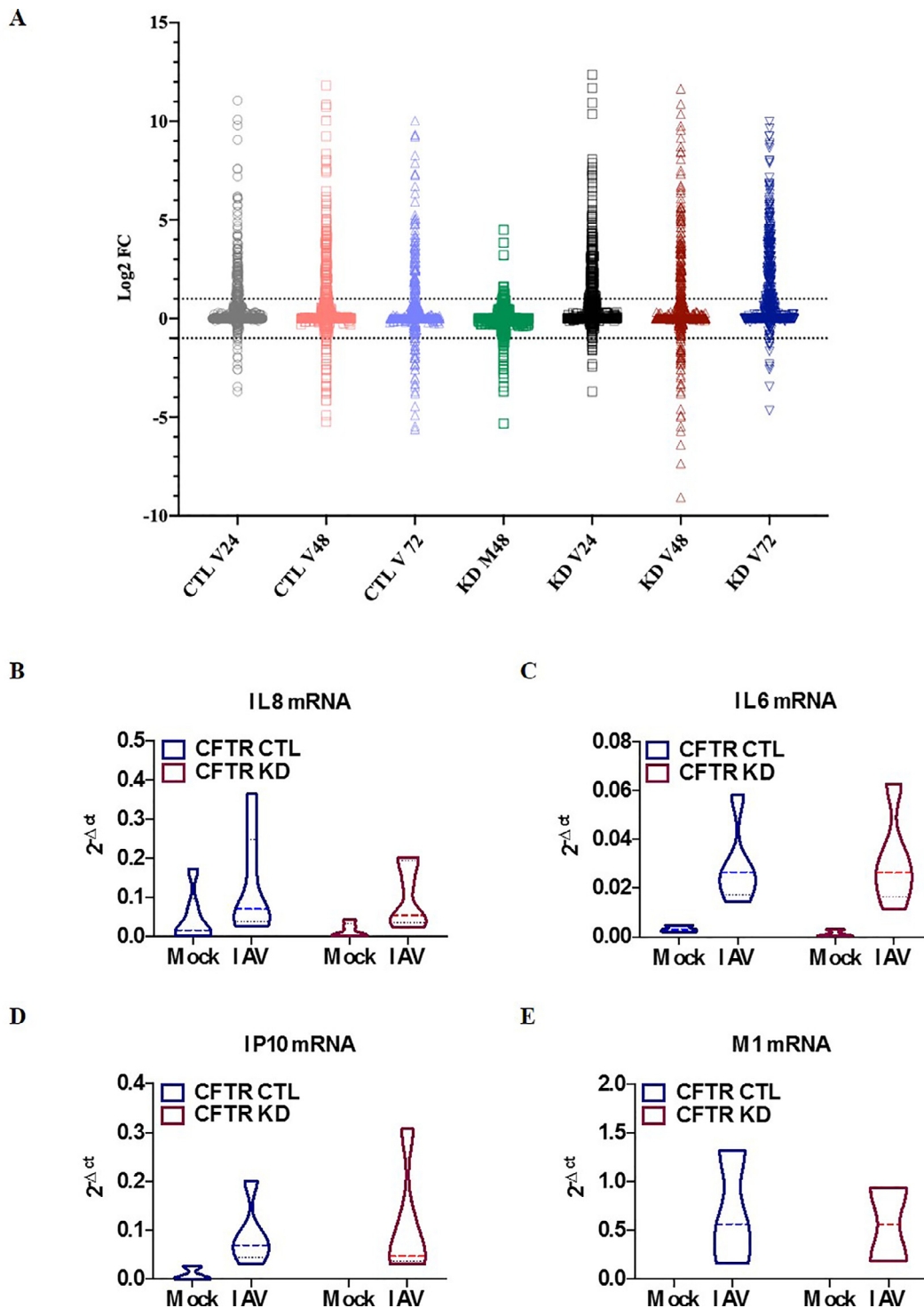


Fig. 3. Immune gene profile of IAV infected CFTR CTL and CFTR KD cells. (A) Dot plots showing distribution of immune gene expression in IAV infected CFTR CTL cells (CTL V) at time points 24, 48, 72 hpi (V24, V48, V72) and IAV infected CFTR KD cells (KD V) at time points 24, 48, 72 hpi (V24, V48, V72) normalized to CFTR CTL mock (CTL Mock). (B) Violin plot of IL8 mRNA expression, (C) IL6 mRNA expression and (E) IAV matrix protein M1 mRNA expression in Mock and IAV infected CFTR CTL (blue) and CFTR KD (red) cells. No difference in gene expression shown in B-E was observed between both cell types. (For interpretation of the references to color in this figure legend, the reader is referred to the web version of this article).

by our GSEA of CFTR CTL and CFTR KD cells exposed to flagellin (Fig. 1G). To determine if CFTR inactivation directly affect IFN-dependent signaling pathways in Calu-3 cells, we also performed NANOSTRING analysis on cells stimulated with different types of IFN, including IFN- α 2B (Type I), IFN- γ (Type II) and IFN- λ 3 (Type III). We first verified the efficiency of the stimulation of CFTR CTL and CFTR KD cells by measuring IP10/CXCL10 mRNA levels, which were similar in response to all three types of IFN (Supplementary

Fig. 3). Supplementary Table 4 shows all gene expression changes in CFTR CTL and CFTR KD cells stimulated with IFN- α 2B, IFN- λ 3 and IFN- γ . Genes of interest are highlighted in the heatmap shown in Fig. 4B, suggesting that CFTR silencing is associated with altered IFN signaling.

Type I and type III are IFNs are released by IAV-infected airway epithelial cells. To gain information on the potential factors regulating the expression of the immune genes, genes modulated

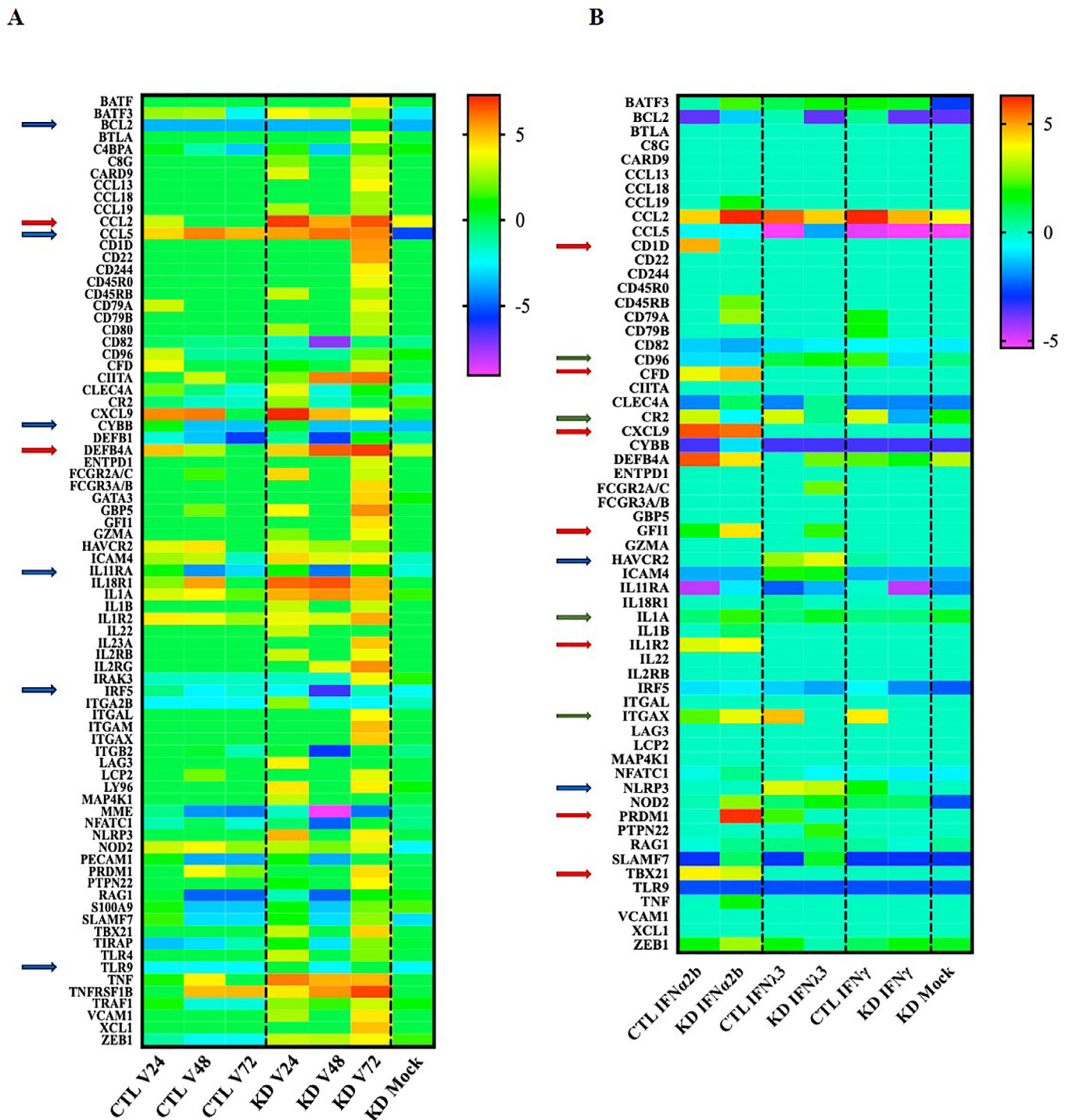
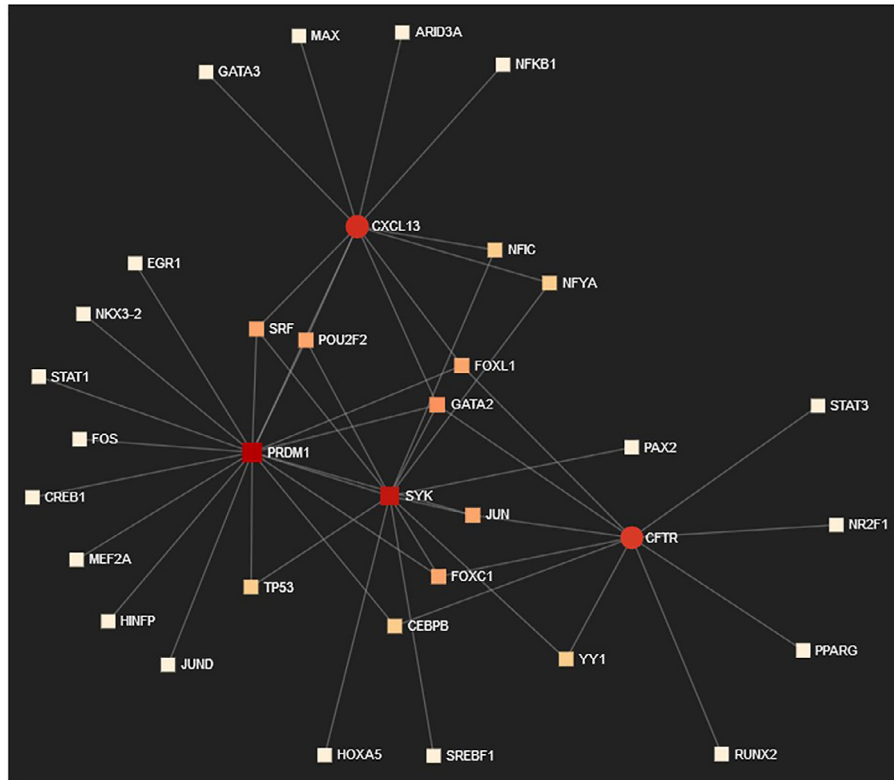


Fig. 4. Heat map profiles of dysregulated genes in IAV infected and IFN stimulated CFTR CTL and CFTR KD cells. (A) Heat map showing selected immunology related genes and expression in IAV infected (CTL V24, V48 and V72, KD V24, V48, V72 and KD Mock) normalized to CTL Mock. Blue arrows point to some genes whose expression was affected by CFTR silencing under uninfected condition. Red arrows indicate genes whose expression is differently affected by IAV infection in CFTR CTL and CFTR KD cells. (B) Heat map showing selected immunology related genes and expression in CFTR CTL and CFTR KD cells with IFN- α 2b, IFN- λ 3 and IFN- γ stimulation, normalized to CTL Mock. Red arrows indicate IFN- α 2b dependent genes, blue arrows indicate IFN- λ 3 dependent genes, and green arrows indicate genes affected by all IFN types (Type I, II and III). Gene expression values are in log₂ scale. (For interpretation of the references to color in this figure legend, the reader is referred to the web version of this article).

by IFN- α 2B and IFN- λ 3 were subjected to a “transcription factor network” analysis. To this end, differentially expressed genes by IFNs between CFTR CTL and CFTR KD cells were uploaded in the NetworkAnalyst software to interrogate the Reactome repositories regarding potential interactions with *CFTR*. The analysis revealed the interaction between hubs of genes constituted of *CFTR*, *SYK*, *PRDM1* and *CXCL13/BCLC* for IFN- α 2B (Fig. 5A) and IFN- λ 3 (Supple-

mentary Figure 4A) stimulations. The figure captions (Fig. 5A and Supplementary Fig. 4A) indicate the transcriptions factors known to interact with these genes, directly or indirectly. These transcription factors, as well as their gene targets in the NANOSTRING gene panels, are listed in Fig. 5B for IFN- α 2B and in Supplementary Figure 4B for IFN- λ 3. A good relationship was observed with changes in gene expression in KD CFTR cells (up and down) de-

A



B

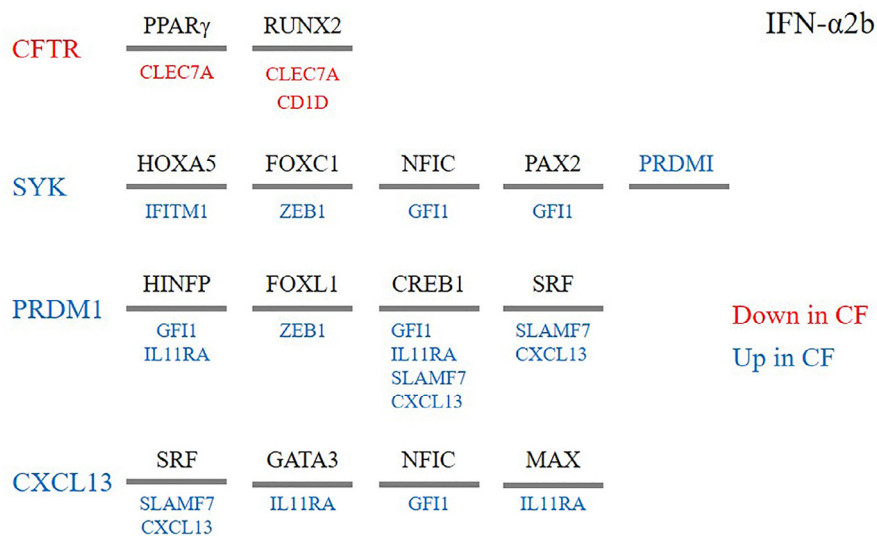


Fig. 5. (A) Figure caption of transcription factor network revealed with NetworkAnalyst (<http://www.networkanalyst.ca/>), which identified SYK, PRDM1 and CXCL13 as hub genes interacting with CFTR. The network of transcription factors regulating the expression of these hub genes is indicated. (B) The hub genes (CFTR, SYK, PRDM1 and CXCL13) and their associated transcription factors for IFN- α 2B stimulation are highlighted. Next to each hub gene are indicated the transcription factors known to regulate their activity. Each transcription factor is visualized by a horizontal bar with its identity indicated on top. Below the bars are listed other target genes of these transcription factors. Whether hub and target genes were down- or upregulated, as revealed by NANOSTRING, is indicated (red, downregulated in CF; blue, upregulated in CF) PRDM1 is as a hub gene and a transcription factor. (For interpretation of the references to color in this figure legend, the reader is referred to the web version of this article.)

tected by NANOSTRING approach for both IFN- α 2B (Fig. 5B) and IFN- λ 3 (Supplementary Fig. 4B). For example, in Fig. 5B, CFTR is transcriptionally regulated by PPAR γ and RUNX2, which serve as transcriptions factors for CLEC7A and CD1D. In CFTR KD cells, both genes are downregulated. In contrast, SYK, PRDM1 and CXCL13 are upregulated in CFTR KD cells as well as other target genes. The results highlight complex immune gene transcriptional net-

work regulation and suggest that IFN signaling is altered in CFTR KD cells.

4. Discussion

We took advantage of a widely used airway epithelial cell line model (Calu-3 cells), where CFTR was inactivated by CRISPR-Cas9

system [8]. Transcriptomic analysis was performed after stimulation with flagellin, which is a potent bacterial virulence factor in the airways of CF patients. Similar to other studies, RNA-seq analysis of CFTR CTL and CFTR KD cells showed that CFTR inhibition primarily affects expression of key genes required for the immune response. The data suggests that CFTR inactivation leads to a pro-inflammatory state in stimulated CFTR KD cells. This was hypothesized in clonal cell lines expressing CFTR to those without [10]. It is interesting to note that these key differences and dysregulation of the immune response are also highlighted in flagellin-stimulated primary cultures of airway epithelial cells from CF and non-CF patients [9].

Flagellin stimulation of Calu-3 cells enhanced pathways involved in viral infection in the bioinformatic analysis, suggesting that our CFTR KD cell model could be useful to investigate the host cell response to viruses. We used a low MOI of infection to preserve the integrity of the airway epithelium grown on Transwell filters and monitored viral growth over time. We did not observe differences in viral replication or particle release between CFTR CTL and CFTR KD cells. However, robust pro-inflammatory response was induced, as evidenced by the *IL-8*, *IL-6* and *IP10* gene transcripts. Multiplex gene expression analysis confirmed the overall immune response of Calu-3 cells infected with IAV, as demonstrated by the enhanced expression of HLA-Class I and II molecules. Of note, genome wide association studies revealed robust signatures for HLA genes with CF disease severity [11].

Multiplex gene array analysis of CFTR inactivated Calu-3 cells revealed downregulated genes of interest that could play a role in the hyperinflammatory state of the CF airways. For example, *BCL2*, a cell death regulator, is downregulated in CFTR KD cells. *BCL2* modulates cell death to variable outcomes for apoptosis, as previously reported in Calu-3 cells and other cell types [12,13]. Interestingly, the dysregulation of the IFN signaling pathway in CFTR KD cells was also observed. *IRF5*, which is a member of the IFN regulatory factor (IRF) family, is downregulated with IAV infection. This group of transcription factors has diverse roles, including virus-mediated activation of IFN, modulation of cell growth, differentiation, apoptosis and immune system activity. *TLR9*, which is expressed within the endosomal compartments, functions to alert the immune system of viral and bacterial infections by binding to DNA rich in CpG motifs. These observations are in line with the finding that there are diminished IFN and IFN-stimulated-gene levels in CF bronchial epithelial cells infected with Rhinovirus [14]. Upregulated genes in CFTR KD cells include the C-C motif chemokine/monocyte attractant *CCL2/MCP1*. Importantly, the expression of *CCL2/MCP1* was strongly induced with IAV in CFTR KD cells. *CCL2/MCP1* was previously shown to be associated with CFTR mutation in pancreatitis-associated disease in CF patients [15] and upregulated in primary cultures of CF airway epithelial cells infected with *P. aeruginosa* [16].

We also observed IAV-dependent genes that were upregulated in the later time points of infection in CFTR KD cells. Among these genes, *CCL13/MCP4*, which is regulated by IL-1 and TNF α , is interesting as the cytokine is reported to be an asthma biomarker [17]. *CD1D*, which helps to present lipid antigens at the cell surface, can activate natural killer T (NKT) cells. When activated, NKT cells rapidly produce cytokines, typically represented by IFN- γ and IL-4 production. *CIITA* encodes the HLA-class II transactivator and has been shown to interact with MAPK1. Although the functional consequences are unknown, the upregulation of a major regulator of HLA-class II molecules may affect antigen presentation by CF airway epithelial cells. Of note, a previous study reported that reduced IFN- γ induced HLA-DQ expression in immune cells from CF patients [18]. In contrast to our results, these authors showed decreased expression of *CIITA*, suggesting that IFN- γ -dependent signaling was impaired in CF. Importantly, IL-4 and IFN- γ were

shown to orchestrate an epithelial polarization in the airways mediated by clustering of transcription factor hubs involving *TBX2* and *ZEB1* [19], two genes that are also upregulated by IAV in our experiments. *NLRP3* is upregulated in our CFTR KD cells during IAV infection, which may contribute to the increased inflammation observed in CFTR KD cells [20]. This is also highlighted by the increased expression of *IL18R1* and *IL1A*, two components of IL-1 signaling that are pro-inflammatory, and of *GBP5*, an activator of the NLRP3 inflammasome. These results are in agreement with the hypothesis that inflammasome-dependent inflammation is enhanced in CF [21,22].

Type I and III IFNs play a major role in the antiviral defense of the airway epithelium. Comparing the “transcription factor network” associated with changes in the expression of the immune genes in CTL and CFTR KD cells stimulated with IFN- α 2B and IFN- λ 3, we found hubs of genes interacting with *CFTR*, namely *SYK*, *PRDM1* and *CXCL13*. *SYK* (spleen tyrosine kinase), a non-receptor tyrosine kinase, has been reported to regulate CFTR localization at the plasma membrane by phosphorylation of residue Y512 [23]. In the presence of pathogens, *SYK* can activate the inflammasome and NF- κ B-mediated transcription of pro-inflammatory mediators [24]. *SYK* is also expressed by lung epithelial cells, thus, *SYK* inhibition has been proposed as a therapeutic strategy for dampening severe inflammation caused by *P. aeruginosa* infection [25]. *SYK* activation was shown to induce the tumor suppressor B-lymphocyte-induced maturation protein-1 (Blimp-1), which is encoded by *PRDM1*, and thought to be a critical regulator of IFN signaling cascades. In mammary epithelial cells, Blimp-1 regulates the expression of viral defense, IFN signaling and MHC class I pathways, and directly targets the transcriptional activator STAT1 [26]. Of note, phosphorylation of STAT1, which activates IFN-mediated signaling was reported to be impaired in CF airway epithelial cells [27].

Both *SYK* and *PRDM1* associate with *CXCL13* through the SRF (serum response factor) and POU2F2 (POU domain, class 2, transcription factor 2) transcription factors. *CXCL13* and its receptor, *CXCR5*, play fundamental roles in inflammatory, infectious and immune responses. It is mostly known to exert important functions in lymphoid neogenesis. In a murine model, expression of *CXCL13* was enriched in lymphoid aggregates that developed in lungs during Respiratory Syncytial virus [28] and persistent *P. aeruginosa* or *S. aureus* airway infection [29].

In summary, our findings reveal target genes in understanding the defective immune response in the CF airway epithelium in the context of viral infection. The results also confirm defective IFN signaling responses that could contribute to the dysregulated tolerance of airway epithelial cells against pathogens. It is however acknowledged that this study only presents predictions from transcriptomic analysis in a simple, though polarized, airway epithelial cell model. Further investigation at the protein level is required to determine and validate the role of the identified genes in the CF airway immune response.

Data availability statement

The datasets analyzed for this study can be found in NCBI Gene Expression Omnibus (GEO) with the accession number GSE133495 <https://identifiers.org/geo:GSE133495>.

Funding

This work was supported by grants from Swiss National Science Foundation (310030_172909), ABCF2 and CFCH to M.C.

Declaration of Competing Interest

The authors declare that the research was conducted in the absence of any commercial or financial relationships that could be construed as a potential conflict of interest.

CRediT authorship contribution statement

Aderonke Sofoluwe: Conceptualization, Methodology, Formal analysis, Investigation, Writing - review & editing. **Alice Zoso:** Formal analysis. **Marc Bacchetta:** Investigation. **Sylvain Lemeille:** Software, Formal analysis, Resources. **Marc Chanson:** Conceptualization, Validation, Writing - original draft, Writing - review & editing, Supervision, Funding acquisition.

Acknowledgments

We would like to thank Didier Chollet, Natacha Civic and Mylène Docquier at the iGE3 Genomics platform (Faculty of Medicine, University of Geneva) for the bioinformatics analysis and Joanna Bou Saab for sample collection in early RNA-seq experiment. We would like to thank Prof. Mirco Schmolke (Department of Microbiology and Molecular Biology, University of Geneva) for the experimental set-up and scientific input. We would also like to thank the University of Geneva, Faculty of Medicine Core Facilities for excellent technical support.

Supplementary materials

Supplementary material associated with this article can be found, in the online version, at [doi:10.1016/j.jcf.2020.08.012](https://doi.org/10.1016/j.jcf.2020.08.012).

References

- [1] Rynda-Applé A, Robinson KM, Alcorn JF. Influenza and bacterial superinfection: illuminating the immunologic mechanisms of disease. *Infect Immun* 2015;83:3764–70. doi:10.1128/IAI.00298-15.
- [2] Wang EE, Prober CG, Manson B, Corey M, Levison H. Association of respiratory viral infections with pulmonary deterioration in patients with cystic fibrosis. *N Engl J Med* 1984;311:1653–8. doi:10.1056/NEJM198412273112602.
- [3] Armstrong D, et al. Severe viral respiratory infections in infants with cystic fibrosis. *Pediatr Pulmonol* 1998;26:371–9. doi:10.1002/(sici)1099-0496(199812)26:6<371::aid-ppul1>3.0.co;2-n.
- [4] Berkebile AR, et al. Airway surface liquid has innate antiviral activity that is reduced in cystic fibrosis. *Am J Respir Cell Mol Biol* 2020;62:104–11. doi:10.1165/rcmb.2018-0304OC.
- [5] Morgan DJ, et al. Innate immune cell suppression and the link with secondary lung bacterial pneumonia. *Front Immunol* 2018;9:2943. doi:10.3389/fimmu.2018.02943.
- [6] Cawcutt K, Kalil AC. Pneumonia with bacterial and viral coinfection. *Curr Opin Crit Care* 2017;23:385–90. doi:10.1097/MCC.0000000000000435.
- [7] Kiedrowski MR, Bomberger JM. Viral-bacterial co-infections in the cystic fibrosis respiratory tract. *Front Immunol* 2018;9:3067. doi:10.3389/fimmu.2018.03067.
- [8] Bellec J, et al. CFTR inactivation by lentiviral vector-mediated RNA interference and CRISPR-Cas9 genome editing in human airway epithelial cells. *Curr Gene Ther* 2015;15:447–59.
- [9] Zoso A, Sofoluwe A, Bacchetta M, Chanson M. Transcriptomic profile of cystic fibrosis airway epithelial cells undergoing repair. *Sci Data* 2019;6:240. doi:10.1038/s41597-019-0256-6.
- [10] Hao S, et al. Inactivation of CFTR by CRISPR/Cas9 alters transcriptional regulation of inflammatory pathways and other networks. *J Cyst Fibros* 2019. doi:10.1016/j.jcf.2019.05.003.
- [11] O'Neal WK, Knowles MR. Cystic fibrosis disease modifiers: complex genetics defines the phenotypic diversity in a monogenic disease. *Annu Rev Genomics Hum Genet* 2018;19:201–22. doi:10.1146/annurev-genom-083117-021329.
- [12] Losa D, et al. Pseudomonas aeruginosa-induced apoptosis in airway epithelial cells is mediated by gap junctional communication in a JNK-dependent manner. *J Immunol* 2014;192:4804–12. doi:10.4049/jimmunol.1301294.
- [13] Chen Q, et al. Cystic fibrosis epithelial cells are primed for apoptosis as a result of increased Fas (CD95). *J Cyst Fibros* 2018;17:616–23. doi:10.1016/j.jcf.2018.01.010.
- [14] Schögler A, et al. Interferon response of the cystic fibrosis bronchial epithelium to major and minor group rhinovirus infection. *J Cyst Fibros* 2016;15:332–9. doi:10.1016/j.jcf.2015.10.013.
- [15] Schwiebert LM, Estell K, Propst SM. Chemokine expression in CF epithelia: implications for the role of CFTR in RANTES expression. *Am J Physiol* 1999;276:C700–10. doi:10.1152/ajpcell.1999.276.3.C700.
- [16] Balloy V, et al. Normal and cystic fibrosis human bronchial epithelial cells infected with pseudomonas aeruginosa exhibit distinct gene activation patterns. *PLoS One* 2015;10:e0140979. doi:10.1371/journal.pone.0140979.
- [17] Kalayci O, et al. Monocyte chemoattractant protein-4 (MCP-4; CCL-13): a biomarker of asthma. *J Asthma* 2004;41:27–33. doi:10.1081/jas-120024590.
- [18] Hofer TP, et al. Decreased expression of HLA-DQ and HLA-DR on cells of the monocytic lineage in cystic fibrosis. *J Mol Med* 2014;92:1293–304. doi:10.1007/s00109-014-1200-z.
- [19] Zissler UM, et al. Interleukin-4 and interferon- γ orchestrate an epithelial polarization in the airways. *Mucosal Immunol* 2016;9:917–26. doi:10.1038/mi.2015.110.
- [20] Scambler T, et al. ENaC-mediated sodium influx exacerbates NLRP3-dependent inflammation in cystic fibrosis. *Elife* 2019;8. doi:10.7554/eLife.49248.
- [21] Rimessi A, et al. Mitochondrial Ca²⁺-dependent NLRP3 activation exacerbates the Pseudomonas aeruginosa-driven inflammatory response in cystic fibrosis. *Nat Commun* 2015;6:6201. doi:10.1038/ncomms7201.
- [22] Iannitti RG, et al. IL-1 receptor antagonist ameliorates inflammasome-dependent inflammation in murine and human cystic fibrosis. *Nat Commun* 2016;7:10791. doi:10.1038/ncomms10791.
- [23] Luz S, et al. Contribution of casein kinase 2 and spleen tyrosine kinase to CFTR trafficking and protein kinase A-induced activity. *Mol Cell Biol* 2011;31:4392–404. doi:10.1128/MCB.05517-11.
- [24] Lin YC, et al. Syk is involved in NLRP3 inflammasome-mediated caspase-1 activation through adaptor ASC phosphorylation and enhanced oligomerization. *J Leukoc Biol* 2015;97:825–35. doi:10.1189/jlb.3HI0814-371RR.
- [25] Alhazmi A, Choi J, Ulanova M. Syk inhibitor R406 downregulates inflammation in an in vitro model of Pseudomonas aeruginosa infection. *Can J Physiol Pharmacol* 2018;96:182–90. doi:10.1139/cjpp-2017-0307.
- [26] Elias S, Robertson EJ, Bikoff EK, Mould AW. Blimp-1/PRDM1 is a critical regulator of Type III Interferon responses in mammary epithelial cells. *Sci Rep* 2018;8:237. doi:10.1038/s41598-017-18652-9.
- [27] Zheng S, et al. Impaired innate host defense causes susceptibility to respiratory virus infections in cystic fibrosis. *Immunity* 2003;18:619–30. doi:10.1016/s1074-7613(03)00114-6.
- [28] Alturaiki W, et al. Expression of the B cell differentiation factor BAFF and chemokine CXCL13 in a murine model of respiratory syncytial virus infection. *Cytokine* 2018;110:267–71. doi:10.1016/j.cyto.2018.01.014.
- [29] Frija-Masson J, et al. Bacteria-driven peribronchial lymphoid neogenesis in bronchiectasis and cystic fibrosis. *Eur Respir J* 2017;49. doi:10.1183/13993003.01873-2016.